Int. J. Electrochem. Sci., 14 **(2019)** 9898 – 9908, doi: 10.20964/2019.10.49

International Journal of ELECTROCHEMICAL SCIENCE
www.electrochemsci.org

Short \Communication

Synthesis of Novel Azophenylbenzotriazole and Its Application as Anode Materials for Lithium Ion Batteries

Shao-hui Sun, Li-ping Duan, Yang-yan Tang, Jun-ming Guo, Xian-hong Ai, Ming-wu Xiang, Rui Wang[1,*]

Yunnan Minzu University, School of Chemistry and Environment, Kunming650000, China
[*]E-mail: chem503@126.com

Received: 4 June 2019 / *Accepted:* 7 August 2019 / *Published:* 30 August 2019

The substitution of renewable organic electrodes for environmentally unfriendly inorganic electrodes is a pivotal link in the development of lithium-ion batteries (LiBs) for large-scale energy storage. Here, we report a new type of organic electrode material based on azophenyl and benzotriazolyl (BTA) groups for LiBs. In view of the easy formation of Cu-BTA complexes in the interface of the copper current collector of LiBs anode, we synthesized azophenylalkylbenzotriazoles, and studied their electrochemical behavior and reaction mechanism as organic electrode materials in LiBs. The synthesized azophenylalkylbenzotriazoles showed the high reversible capacity up to 365.8 $mAhg^{-1}$ at 25 mAg^{-1} of current density.

Keywords: azobenzene; electrode material; copper foil; lithium storage performance; electrochemical performance

1. INTRODUCTION

With the increase in global population and the improvement of living standard in developing countries, the global demand for energy is increasing. Technological advances such as portable electronics and electric cars also have increased energy demand. The majority of energy is supplied by fossil fuels such as coal and oil, but their availability is declining. In addition, the excessive use of fossil fuels may cause environmental problems. The global environment will be changed because of emissions of gases such as carbon monoxide from the burning of fossil fuels. Therefore, the two major challenges of the 21st century are to meet the growing demand for energy and to solve environmental problems. Clean and efficient renewable energy sources such as solar, water and wind are required for overcoming these challenges. As solar and wind energy cannot be available on demand, appropriate storage facilities are needed to optimize the use of these renewable sources. Compared with other rechargeable batteries, lithium ion batteries are characterized by higher energy density and better

recyclability, so lithium ion batteries have attracted wide attention in a variety of applications ranging from portable electronics to electric automobiles.

Though organic materials have been studied for a long time as anode material of lithium battery, the development of conductive polymers as rechargeable cathodes slowed down and interest in organic electrodes declined with the success of inorganic materials in the late 1980s. In recent years, organic electrodes attracted public attention again because a large amount of energy is required to prepare inorganic materials[1,2]. In addition to the theoretical capacity value (usually higher than 400 $mAhg^{-1}$), organic materials can be easily accessible. Compared with inorganic compounds, they do not contain expensive elements and can be recycled. They can be used to design a variety of functional devices, such as all-plastic flexible batteries. In addition, the sufficient purity, crystallinity and electrode properties can be obtained for organic materials without high temperature annealing required by inorganic materials. Therefore, their manufacturing processes are environmentally and economically friendly, and they are ideal substitutes for inorganic materials[3-5]. At present, the following compounds are mainly included in researches on organic compound electrode materials: organic disulfide[6-10]; nitryl radical polymer[11-14]; conjugate carbonyl compounds[15,16] and azo compounds[17,18].

Currently, the application prospect of azobenzene in electrode materials has been proved. Luo et al[17,18] used azobenzene as the electrode material to obtain an initial discharge specific capacity of 153 $mAhg^{-1}$, but the specific capacity was still low. Benzotriazole is a common copper corrosion inhibitor[19], which can forms Cu-BAT complex with copper surface through self-assembly. An increasing number of studies attach great importance to the functional structure constructed through self-assembly[20], which has been used to enhance electrode performance[21], so a novel azophenylbenzotriazole compound (B_n) was designed and synthesized in this study to be further used as the electrode material of a lithium battery, and it was expected that the affinity of benzotriazole with copper helps to increase the specific capacity[22-27]. In this paper, the initial discharge capacities of azophenylbenzotriazole compounds (B_n) at current density of 25 mAg^{-1} were 365.8 $mAhg^{-1}$, 231.9 $mAhg^{-1}$, 201.3 $mAhg^{-1}$, respectively with higher discharge specific capacity. Among them, as the intermediate carbon chain was reduced, the degree of conjugation would increase. When n=2, the discharge specific capacity was the largest with up to 365.8 $mAhg^{-1}$. Finally, the adsorptive performance of azophenylbenzotriazole (B_n) on the surface of copper current collector was studied, which indicated that the adsorption of the compound (B_n) on the surface of the copper current collector is generally considered to be the self-assembly of the compound (B_n) on the surface of the copper current collector to form Cu-B_n complex.

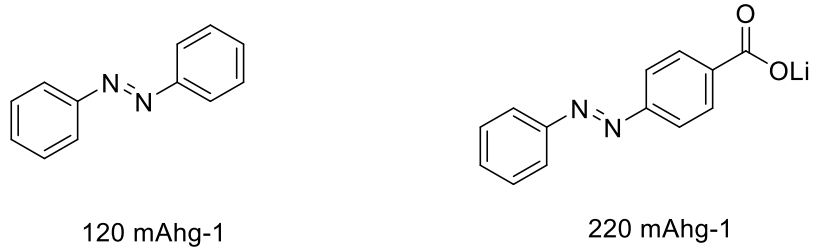

120 mAhg-1 220 mAhg-1

Figure 1. Initial discharge specific capacity of azobenzene compounds as anode materials for lithium battery electrodes as reported in the literature

2. EXPERIMENT

2.1. Organic Synthesis

The molecular structure and synthetic route of the synthesized compounds are shown in the figure 2:

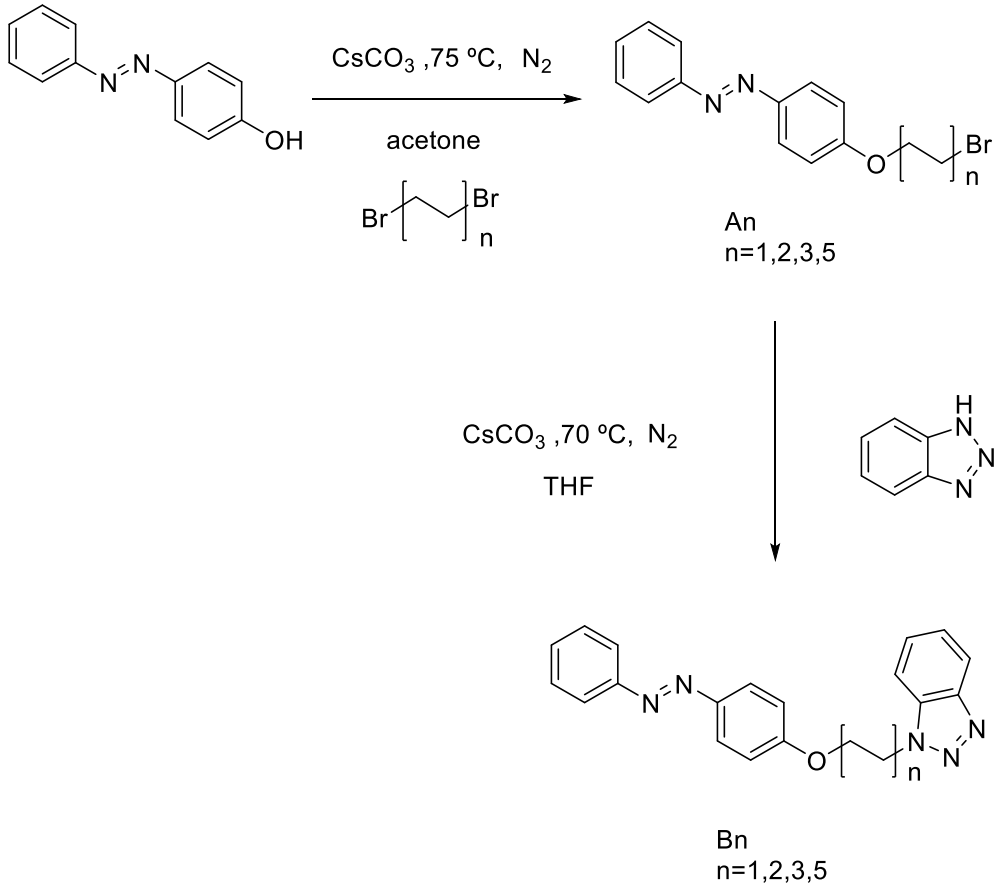

Figure 2. Synthesis route of azophenylbenzotriazole compounds

Synthesis of azophenyl bromide (A_n)

Synthesis and structural characterization of azophenyl (bromoethane) ether (A_1): 5 mmol of P-hydroxy azobenzene, 30 mmol of 1,2-dibromoethane in a 250 mL three-neck bottle, 2 g of cesium carbonate, 80 mL of acetone, reacted under nitrogen atmosphere at 75 ℃ for three days, filtered while hot, spin dried, and recrystallized from ethanol. yellow powder was obtained in a yield of 40%. ^{1}H NMR (400 MHz, $CDCl_3$) δ 8.35–8.31 (m, 2H), 8.02–7.99 (m, 2H), 7.27–7.23 (m, 2H), 6.90–6.87 (m, 2H), 4.50 (t, J = 6.2 Hz, 2H), 3.50 (t, J = 6.3 Hz, 2H).

Synthesis of azophenyl (bromobutane) ether (A_2): The synthesis method was the same as that of A_1, and the yield was 80%. ^{1}H NMR (400 MHz, $CDCl_3$) δ 8.32 (d, J = 9.0 Hz, 2H), 8.01 (d, J = 8.5 Hz, 2H), 7.27–7.23 (m, 2H), 6.89–6.86 (m, 2H) , 4.29 (t, J = 6.9 Hz, 2H), 3.27 (t, J = 6.7 Hz, 2H), 1.90–1.77 (m, 4H).

Synthesis of azophenyl (bromohexane) ether (A_3): The synthesis method was the same as that of A_1, and the yield was 81%. ^{1}H NMR (400 MHz, $CDCl_3$) δ 8.34–8.30 (m, 2H), 8.02–7.99 (m, 2H), 7.27–7.23 (m, 2H), 6.89–6.86 (m, 2H), 4.28 (t, J = 6.8 Hz, 2H), 3.26 (t, J = 6.8 Hz, 2H), 1.82 (dp, J =

11.3, 7.2 Hz, 4H), 1.38–1.26 (m, 4H).

Synthesis of azophenyl (bromoaralkyl) ether (A_5): The synthesis method was the same as that of A1, and the yield was 83%. 1H NMR (400 MHz, $CDCl_3$) δ 8.34–8.31 (m, 2H), 8.02–7.99 (m, 2H), 7.26–7.23 (m, 2H), 6.90–6.86 (m, 2H), 4.28 (t, J = 6.8 Hz, 2H), 3.26 (t, J = 6.8 Hz, 2H), 1.86–1.76 (m, 4H), 1.42–1.21 (m, 12H).

Synthesis of azophenylbenzotriazole Compound B_n

Synthesis and characterization of B_1: 1 mmol of product B_1, 1.1 mmol of benzotriazole in a 50 mL two-necked flask, 2 mmol of cesium carbonate, 10 mL of tetrahydrofuran, and reacted under nitrogen atmosphere at 70 °C for three days, and extracted. Dry, PE: EA passed through the column, yield: 70%. ^{1}H NMR (400 MHz, DMSO) δ 8.34-8.31 (m, 2H), 8.03-7.94 (m, 3H), 7.84-7.75 (m, 2H), 7.27-7.21 (m, 3H), 6.88 (d, J = 8.7 Hz, 2H), 4.71 (t, J = 6.3 Hz, 2H), 4.32 (t, J = 6.2 Hz, 2H).

Synthesis and characterization of B_2: The synthesis method was the same as that of B_1, and the yield was 72%. ^{1}H NMR (400 MHz, DMSO) δ 8.39-8.28 (m, 2H), 8.03-7.94 (m, 3H), 7.79 (ddt, J = 16.4, 8.2, 4.3 Hz, 2H), 7.30–7.21 (m, 3H), 6.91–6.81 (m, 2H), 4.43 (t, J = 6.5 Hz, 2H), 4.30 (t, J = 6.8 Hz, 2H), 2.00 (dd, J = 13.4, 6.7 Hz, 2H), 1.91–1.83 (m, 2H).

Synthesis and characterization of B_3: The synthesis method was the same as that of B_1, and the yield was 71%. ^{1}H NMR (400 MHz, DMSO) δ 8.34–8.31 (m, 2H), 8.02–7.94 (m, 3H), 7.83–7.74 (m, 2H), 7.26–7.21 (m, 3H), 6.89–6.86 (m , 2H), 4.45 (t, J = 6.3 Hz, 2H), 4.28 (t, J = 7.0 Hz, 2H), 1.96 (p, J = 6.7 Hz, 2H), 1.84 (dd, J = 14.5, 7.3 Hz , 2H), 1.36–1.24 (m, 4H).

Synthesis and characterization of B_5: The synthesis method was the same as that of B_1, and the yield was 75%. ^{1}H NMR (400 MHz, DMSO) δ 8.34–8.30 (m, 2H), 8.02–7.94 (m, 3H), 7.79 (dtd, J = 9.6, 8.0, 1.6 Hz, 2H), 7.27–7.21 (m, 3H), 6.90–6.86 (m, 2H), 4.45 (t, J = 6.3 Hz, 2H), 4.28 (t, J = 6.8 Hz, 2H), 1.95 (p, J = 6.5 Hz, 2H), 1.87–1.79 (m, 2H), 1.41–1.21 (m, 12H).

2.2 Preparation of electrodes and assembly of batteries

CR2025 analog coin cell battery that facilitates specific capacity and cycle performance test of electrode materials is used in the lab. Before the battery is assembled, the positive electrode shell, foamed nickel and negative electrode case should be placed in a drying oven at 120 °C for 12 hours. The lithium sheet acts as the reference electrode and the counter electrode, the polypropylene microporous film Celgard 2032 as the separator, the prepared negative electrode sheet as the working electrode, and the EC+DMC (volume ratio 1:1) of 1 mol/L $LiPF_6$ as the electrolyte, which is filled with high purity. The components were assembled in sequence for the components in an argon vacuum glove box (both oxygen content and water content less than 1 ppm)

Firstly, CMC (N-methylcellulose binder) and conductive carbon black were uniformly ground in an agate mortar. The anode material to be tested was added after around 30 minutes and the compound was further ground for about 30 minutes. Then, the evenly mixed slurry was evenly coated on the cut copper foil with a medicine spoon, placed in a blast drying oven at 60 ° C. After drying, the pole piece was cut into 15 mm regular discs and weighed on a precision balance. Then, it was placed in a vacuum drying oven and dried at a constant temperature of 60 °C. The working pole piece of the lithium ion battery was then stored in the glove box for further use.

The assembly process of the lithium ion battery is as follows: the metal Li piece acts as the counter electrode and the battery is assembled in the glove box. The assembly order of the battery parts

is as follows: the negative electrode case, the Li piece, the electrolyte, the separator, the electrolyte, the electrode, the electrode, and the positive electrode (from top to bottom).

3. RESULTS AND DISCUSSION

3.1. Structural characterization of a novel azobenzenebenzotriazole compound (B_n)

Firstly, azophenyl bromide (A_n) was synthesized by an ether formation reaction. The benzotriazole-modified azobenzene compound (B_n) was prepared by nucleophilic substitution of benzotriazole and A_n. The molecular structure of all newly synthesized compounds was characterized by means of nuclear magnetic resonance and Fourier transform infrared spectroscopy, and it was proved that the synthesized molecular structure was consistent with the design.

Figure 3 is an infrared spectrum of a novel azophenylbenzotriazole compound after tableting.3429 cm^{-1} corresponds to the peak of water absorbed by the sample, 2980-2850 cm^{-1} corresponds to the stretching vibration in CH_2 and CH_3, 2400-2300 cm^{-1} to the peak of CO_2 in the air, and 1600-1450 cm^{-1} to the vibration of the benzene ring skeleton, 1337 cm^{-1} to CH_2 out-of-plane sway, 1255-1016 cm^{-1} to CO stretching vibration, and 600-740 cm^{-1} to benzene ring CH out-of-plane bending vibration. However, e new characteristic functional groups will not be produced as chain length increases, and no significant change is observed from the infrared spectrum. It is necessary to combine the nuclear magnetic data mentioned in the above section to prove that the obtained molecules are consistent with the design.

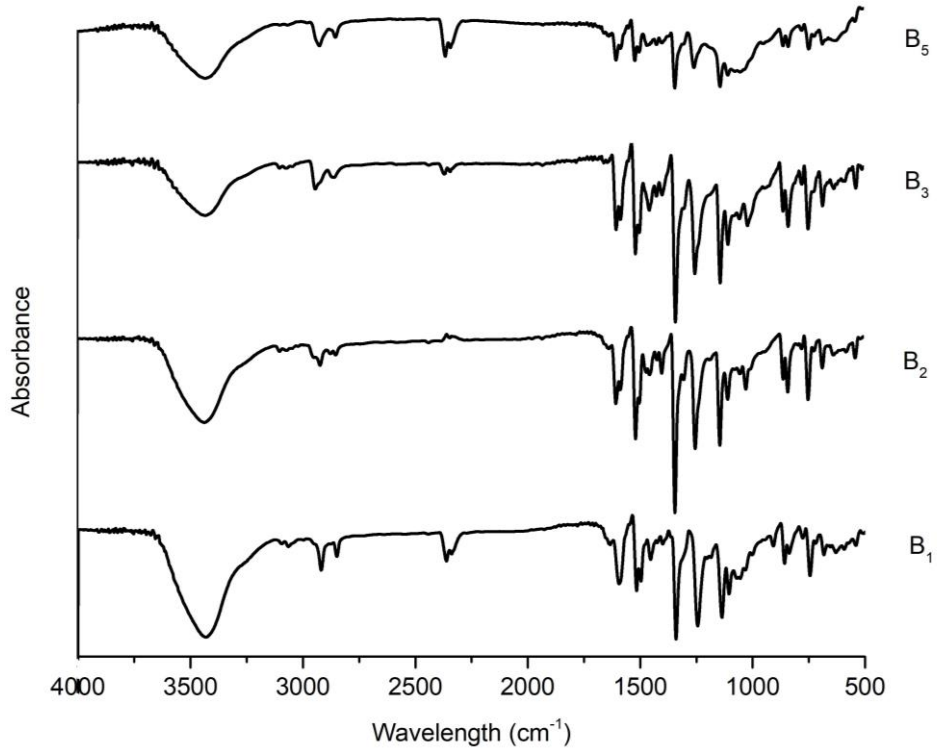

Figure 3. Infrared absorption spectrum of a novel azophenylbenzotriazole compound (B_n)

3.2. Cyclic voltammetry

To determine the redox process of the compound, the electrode material was subjected to cyclic voltammetry (Fig. 4) and scanned at a rate of 0.5 mVs^{-1}, where B_2 had two discharge platforms of 1.35 V and 1.95 V; two of 2.8 V and 3.1 V Charging platform; B_3 had two discharge platforms of 1.25 V and 1.55 V; two charging platforms of 2.4 V and 2.6 V; B_5 had two discharge platforms of 1.2 V and 1.6 V; two charging platforms of 2.2 V and 2.6 V; The redox reaction was a two-step reaction; since the peak-to-peak voltage difference was too large, the reversibility of redox was poor, and the first discharge capacity was much larger than the charge capacity. The reason for the large difference in the first charge and discharge might be that the synthesized organic matter was in solution during the battery cycle.

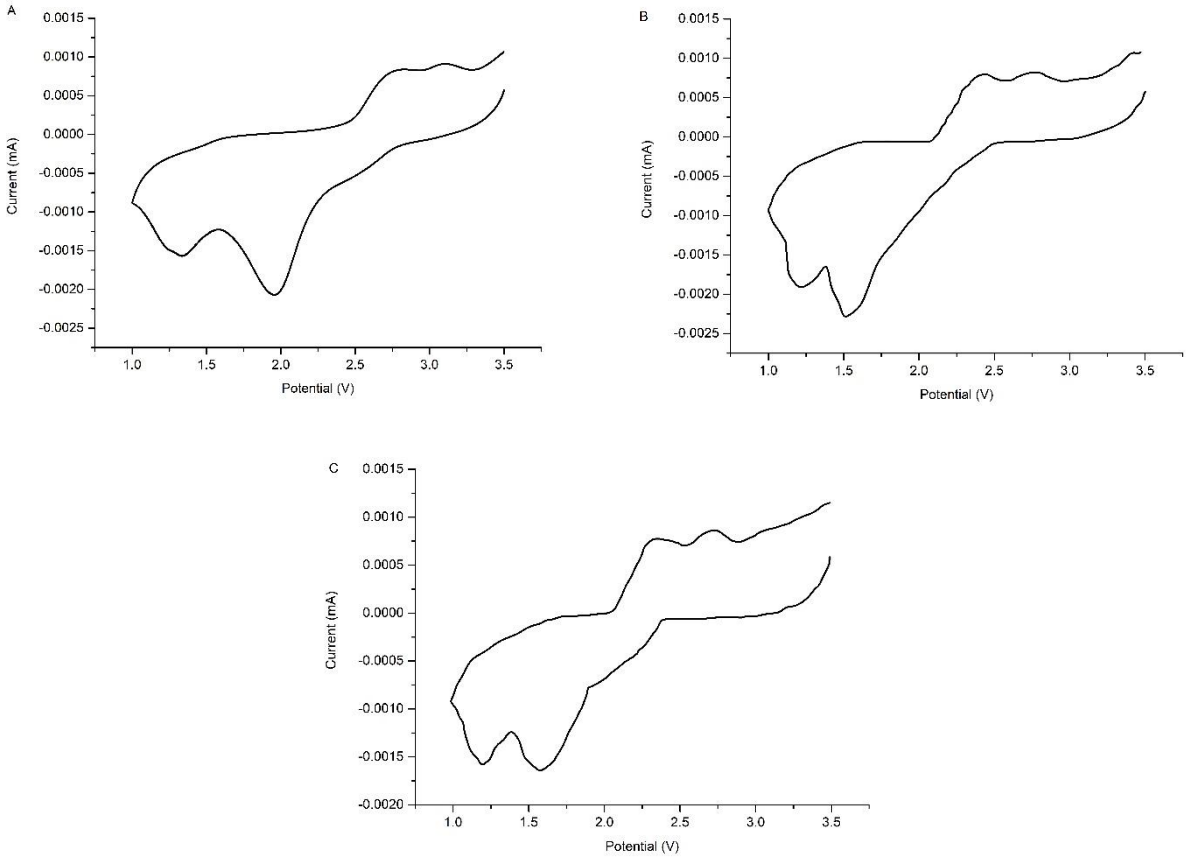

Figure 4. A) Cyclic voltammogram of the negative electrode sheet of the compound B_2 as the active material; B) the cyclic voltammogram of the negative electrode sheet of the compound B_3 as the active material; C) the cyclic voltammogram of the negative electrode sheet of the compound B_5 as the active material

Based on the above analysis, we describe the mechanism of this series of compounds, as shown in Figure 5:

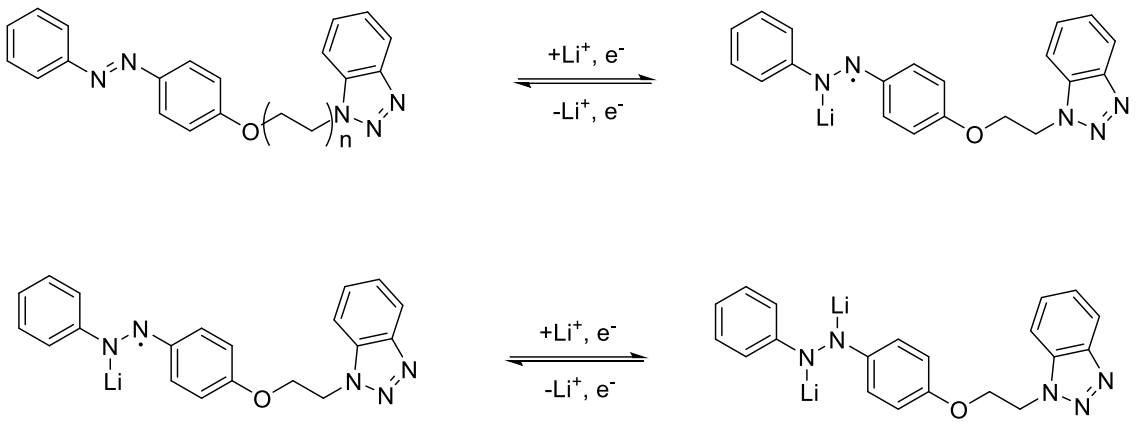

Figure 5. Redox reaction of electrode materials with active compounds B_2, B_3 and B_5

3.3 Lithium storage performance of azophenylbenzotriazole compounds

The lithium storage performance of the compound is acquired by constant current charge and discharge. We will analyze the charge and discharge performance of these three lithium ion battery anodes with B_2, B_3 and B_5 compounds as active substances in the following sections.

Firstly, the benzotriazole introduced by us has been proved to have an adsorption property[22] on the copper current collector. It is speculated that the surface coordination of BTAH on the Cu surface involves a chemisorption layer or a BTA polymer film. BTAH exhibits different adsorption and filming behaviors in different potential regions of the solution. Therefore, we introduced benzotriazole as a part of the electrode material; likewise, azobenzene has been proved to have a promising application in electrode materials of lithium ion[22], so it is introduced as another part of the electrode material. As shown in Figure 6, at a current density of 25 mAg^{-1}, compounds B_2, B_3, and B_5 were used as electrode materials of lithium ion, and the initial discharge capacities were 365.8 $mAhg^{-1}$, 231.9 $mAhg^{-1}$, and 201.3 $mAhg^{-1}$, respectively. They were 30.9 %, 43.7%, and 45.5%, respectively, which were consistent with the results obtained by cyclic voltammetry; the Coulomb efficiency of the second cycle increased to 70.5 %, 71.4 %, and 83 %, respectively, and the specific discharge capacity decreased to 156.9. $mAhg^{-1}$, 115.9 $mAhg^{-1}$, 103.8 $mAhg^{-1}$, the Coulomb efficiency remained at 73%, 75%, 80% in the subsequent 40 cycles, but the charge and discharge capacity attenuation was greater; the discharge capacity was attenuated to 127.7 $mAhg^{-1}$, 82.1 $mAhg^{-1}$, and 82 $mAhg^{-1}$, respectively, and the charge capacity was attenuated to 103.1 $mAhg^{-1}$, 63.2 $mAhg^{-1}$, and 73 $mAhg^{-1}$, respectively in the fourth cycle. Its structural frame was more rigid and has better lithium storage performance. The best discharge specific capacity could reach 365.8 $mAhg^{-1}$. As a new type of electrode material, azobenzene is known in the literature [17]. The best specific discharge capacity is 220 $mAhg^{-1}$, and the initial coulombic efficiency is only 27.3%; although our initial coulombic efficiency is also low. However, we have improved the discharge specific capacity and greatly increased the discharge specific capacity, but there are also shortcomings, that is, the cycle efficiency is smaller than that reported in the literature, and this is the place that needs to be broken later.

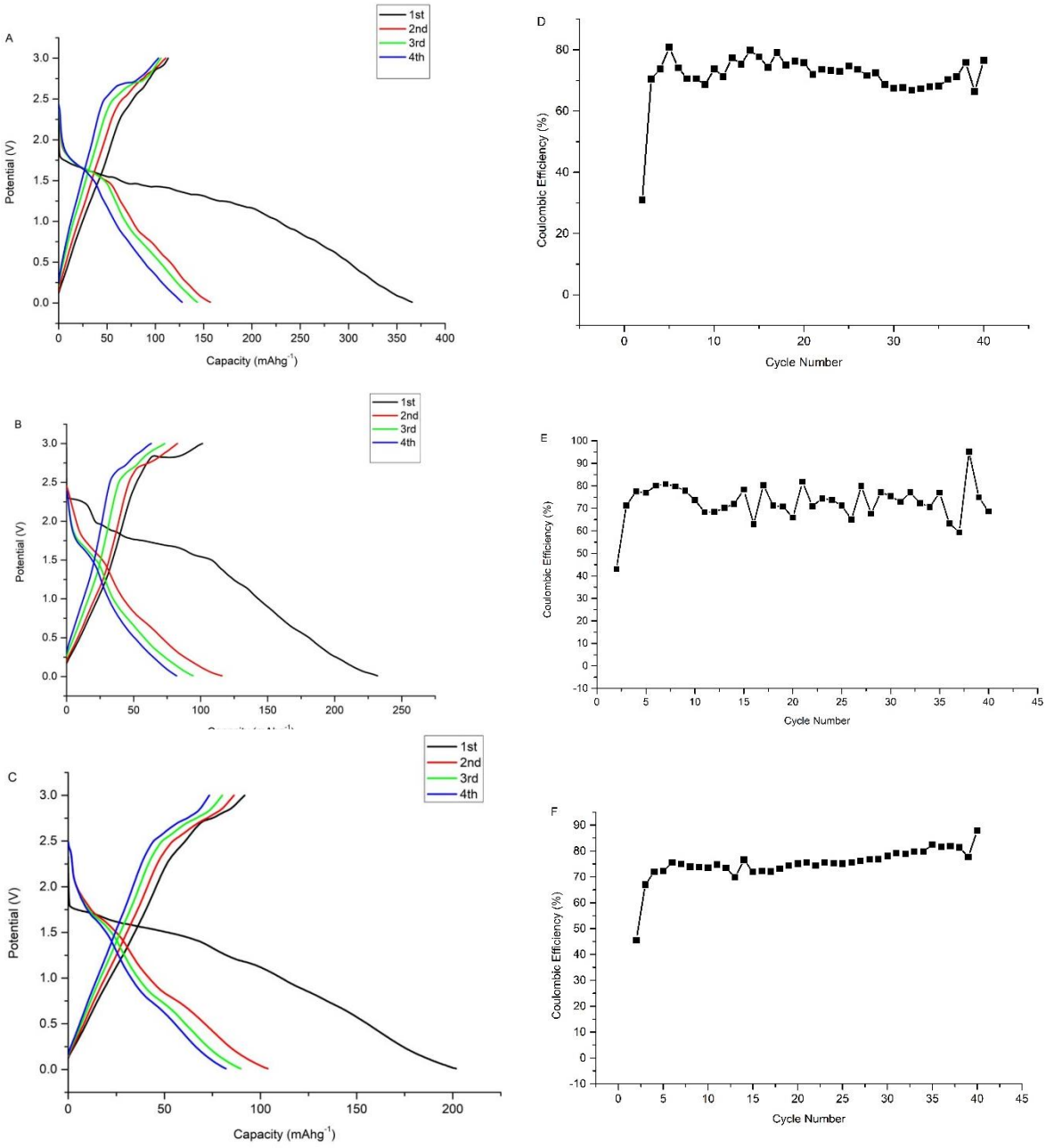

Figure 6. A), B), C) is The constant current charge and discharge of B_2, B_3 and B_5 compound as active materials of the lithium ion battery anode material in the first, second, third, and fourth cycles; D), E), F) is coulombic efficiency of lithium ion battery anode materials with B_2, B_3 and B_5 compounds as active substances in the first 40 cycles of

In Fig 7, in the 40th cycle, the discharge capacity was attenuated to 68.1 $mAhg^{-1}$, 57.6 $mAhg^{-1}$, and 55.2 $mAhg^{-1}$, respectively, and the charge capacity was attenuated to 46.1 $mAhg^{-1}$, 38.1 $mAhg^{-1}$, and 36.3 $mAhg^{-1}$, respectively. The capacity loss might be caused by the decomposition of the electrolyte, formation of the SEI film or some other irreversible reactions[28].

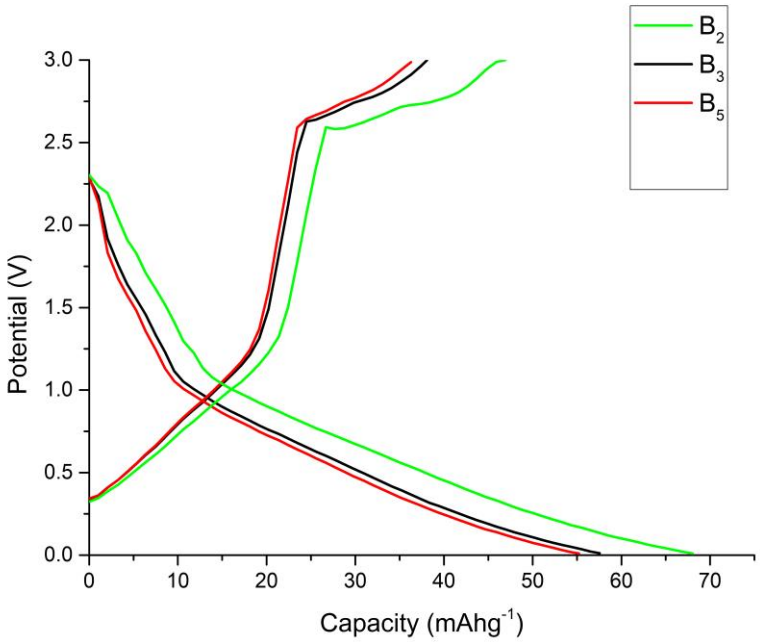

Figure 7. The constant current charge and discharge of B_2, B_3 and B_5 compound as active materials of the lithium ion battery anode material in the first, second, third, and fourth cycles;

3.4 Adsorption of Electrode Materials on Copper Current Collectors

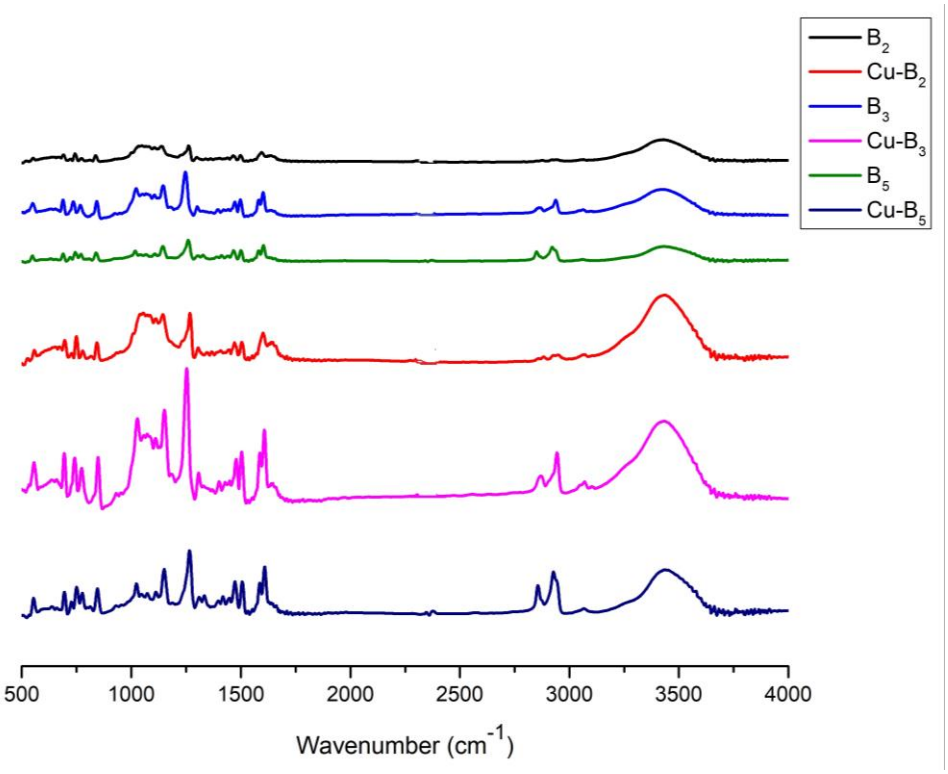

Figure 8. Raman spectra of compounds B_2, B_3 and B_5 solids and their SERS spectra when adsorbed on a copper electrode with a potential of 0.2 V

As shown in Fig 8, the Raman spectra of the solids of the compounds B_2, B_3 and B_5 were compared with the SERS spectra of the surface of the copper electrode at a potential of 0.2 V. It was found that there were significant differences, indicating that the compounds B_2, B_3 and B_5 have a certain effect when on the surface of the copper electrode and are adsorbed on the surface of the copper electrode, which is generally considered to be the self-assembly of the compound (B_n) on the surface of the copper current collector to form Cu-B_n complex.

4. CONCLUSIONS

In summary, the potential value of azophenylbenzotriazole compounds in electrode materials for lithium ion battery is demonstrated. It is expected that the electrode materials will coordinate with the copper current collectors to increase the specific capacity, but certain problems may occur. The biggest problem is that the solubility of the electrode material in the electrolyte, which can be achieved by changing the electrolyte of the lithium ion battery in the future, but there is still a large room for commercialization.

ACKNOWLEDGMENTS
Shao-hui Sun thank the CONACYT (China) for the financial support given to realize their postgraduate studies

CONFLICT OF INTERESTS
The authors declare that there is no conflict of interests regarding the publication of this paper.

References

1. C.P. Grey, J.M. Tarascon, *Nature Materials*, 16 (2016) 45.
2. D. Larcher, J.M. Tarascon, *Nature Chemistry*, 7 (2015) 19.
3. Y. Xu, C. Zhang and M. Zhou, *Nature Communications*, 9(2018) 1720.
4. S. Muench, A. Wild, C. Friebe, B. Hupler, T. Janoschka, U.S. Schubert, *Chemical Reviews*,116 (2016) 9438.
5. Y. Liang, Z. Tao, J. Chen, *Advanced Energy Materials*, 2 (2012) 742.
6. S.J. Visco, L.C. Dejonghe, *Journal of The Electrochemical Society*, 135(1988) 2905.
7. S.J. Visco, M. Liu, L.C. DeJonghe, *Journal of the Electrochemical Society*, 137 (1989) 1191.
8. M. Liu, S.J. Visco, L.C. Dejonghe, *Journal of the Electrochemical Society*, 138 (1989) 1891.
9. K. Naoi, K. Kawase, *Mrs Proceedings*, 496 (1997) L173.
10. S.R. Deng, L.B. Kong, G.Q. Hu, T. Wu, D. Li, Y.H. Zhou, Z.Y. Li, *Electrochimica Acta*, 51 (2006) 2589.
11. K. Nakahara, S. Iwasa, M. Satoh, Y. Morioka, J. Iriyama, M. Suguro, E. Hasegawa, *Chemical Physics Letters*, 359 (2002) 351.
12. T. Suga, H. Konishi, H. Nishide, *Chemical Communications*, 43 (2007) 1730.
13. N. Chikushi, H. Yamada, K. Oyaizu, H. Nishide, *Science China Chemistry*, 55 (2012) 822.
14. K. Oyaizu, T. Kawamoto, T. Suga, H. Nishide, *Macromolecules*, 43 (2010) 10382.
15. X. Jian, P. Gu, Q. Zhang, *Acs Energy Letters*, 2 (2017) 1985.
16. J. Xie, Q. Zhang, *Journal of Materials Chemistry A*, 4 (2016) 7091.

17. C. Luo, X. Ji, S. Hou, N. Eidson, X. Fan, Y. Liang, T. Deng, J. Jiang, C. Wang, *Advanced Materials*, 30 (2018) 1706498.
18. L. Chao, G. L. Xu, J. Xiao, S. Hou, C. Long, W. Fei, J. Jiang, Z. Chen, R. Yang, K. Amine, *Angewandte Chemie International Edition*, 130 (2018)2879.
19. M.M. Antonijevic and M.B. Petrovic, *International Journal of Electrochemical Science*, 3 (2008) 1
20. C. Fang, H. Zhu, O. Chen, M.B. Zimmt, *Chemical communications*, 54(2018)8056.
21. W. Yang, T. Li, H. Zhou, H. Zheng, C. Fu, C. Liang, M. Li, Y. Kuang, *Electrochimica Acta*, 220 (2016) 245.
22. Y.I. Yuan, P.I. Wei, W. Qin, Y. Zhang, R. Gu, *European Journal of Inorganic Chemistry*, 2007 (2010) 4980.
23. T.E. Furtak, J. Kester, *Physical Review Letters*, 45 (1980) 1652.
24. P.G. Cao, J.L. Yao, J.W. Zheng, R.A. Gu, Z.Q. Tian, *Langmuir*, 18 (2001) 100.
25. P. Cao, R. Gu, Z. Tian, *Langmuir*, 18 (2002) 7609.
26. J.L. Yao, B. Ren, Z.F. Huang, P.G. Cao, R.A. Gu, Z.Q. Tian, *Electrochimica Acta*, 48 (2003) 1263.
27. C.J. Milios, E. Manessi-Zoupa, S.P. Perlepes, A. Terzis, C.P. Raptopoulou, *Transition Metal Chemistry*, 27 (2002) 864.
28. V.A. Mihali, S. Renault, L. Nyholm, D. Brandell, *Rsc Advances*, 4 (2014) 38004.